Field Trial of Autonomous Lightpath Provisioning over an SDM Network using 7-Core Fibers

Xiaoliang Chen, *Senior Member, IEEE*, Hanyu Gao, Xin Xiong, Xuefeng Yan, Zuqing Zhu, *Fellow, IEEE*, and Zhaohui Li

(Post-Deadline Paper)

***Abstract*—This paper demonstrates the first field trial of autonomous lightpath provisioning over a space-division multiplexing (SDM) optical network built with 16.5-km 7-core fibers. In particular, we devised an amplifier gain configuration algorithm aided by a composable quality-of-transmission (QoT) estimator. The composable QoT estimator allows per-span impairment assessment, and therefore, enables sequential gain optimization without the need for data plane trial and error. For each amplifier, the algorithm picks a solution that maximizes the overall QoT margin obtained for both in-service and newly established lightpaths. We trained the QoT estimator with data collected from the field testbed and conducted lightpath provisioning experiments under multiple scenarios (using different routing, modulation formats and baud rates). We also demonstrated automated failover operations in the cases of equipment failure and receiver filter shifting. Results show that the proposed design can accomplish lightpath configuration/failover autonomously in around 10 seconds while securing desired QoT levels.**

***Index Terms*—Field trial, space-division multiplexing, 7-core fibers, amplifier gain configuration, composable machine learning.**

I. Introduction

The prevailing of novel networking paradigms and applications, such as big data analytics, has led to continuous inflation of global traffic, posing greater challenges to the underlying transport networks. Recently, space-division multiplexing (SDM) optical networks are emerging as appealing candidates for meeting such challenges [1]. By fully exploiting the spatial and frequency channels in multi-core and/or multi-mode fibers (MCFs/MMFs), recent progresses have reported multi-Petabit/s capacities over single fibers [2].

While SDM offers larger link capacities, the extended resource dimensions (fiber/core/mode/frequency) [3] and the complicated interplay between spatial channels [e.g., inter-core crosstalk (IC-XT)] [4] make the optimization of service provisioning in such networks nontrivial. In this context, extensive research endeavors have been made to develop flexible SDM node/switching architectures [5]–[7], software-defined networking (SDN) based control and management [8], optical performance monitoring/assurance techniques [9], and crosstalk-aware core and spectrum allocation policies [10]–[13]. However, most of these works evaluate IC-XT with analytical models and employ rule-based heuristic resource allocation approaches, which may suffer from poor estimation accuracy or resource utilization.

Lately, with several profound advances, especially in the deep learning domain, machine learning (ML) has revived as promising alternatives or complements to conventional optimization methods for optical communications. Combining ML with SDN technologies, optical network operators can potentially realize autonomous networking with minimal human intervention [14], [15]. Previous works have demonstrated successful applications of ML in various tasks, including quality-of-transmission (QoT) estimation [16]–[18], wavelength configuration [19]–[21], resource allocation [22], [23], and fault management [24]–[26] etc.

Despite the promising prospect of the existing ML-based designs, they mostly rely on simulation or experimental data/environment that can hardly fully reflect realistic optical networks. In [20], the authors demonstrated autonomous wavelength configuration on a real-world backbone network using a Bayesian optimization method. Similar to the work in [21], their approach is built on repeated data plane trial and error, which will inevitably interfere in-service connections and lead to prolonged configuration period. Nevertheless, the work presented in [20] concentrates on optimizing a legacy optical network, and to the best of our knowledge, few study has reported autonomous service provisioning trials in field SDM environments.

In this work, we demonstrate autonomous lightpath provisioning over a field-deployed SDM network using 7-core fibers. By virtue of composable ML's capability of per-span impairment assessment, we developed an algorithm that can dynamically optimize the amplifier gains without intervening data plane operations. This paper extends the previous work in [27] by (*i*) providing more detailed descriptions about the field testbed, the composable QoT estimator, and the amplifier gain configuration algorithm, and (*ii*) presenting enhanced experimental results with a larger data set and additional lightpath provisioning and failover scenarios. The results verify the effectiveness of the proposed design.

The rest of the paper is organized as follows. Section II briefly reviews the state of the art on SDM networking and ML applications for optical networks. In Section III, we elaborate on the field-deployed SDM testbed, including the data and

X. Chen, H. Gao and Z. Li are with the School of Electronics and Information Technology & Guangdong Provincial Key Labratory of Optoelectronic Information Processing Chips and Systems, Sun Yat-sen University, Guangzhou, China, and Southern Marine Science and Engineering Guangdong Laboratory, Zhuhai, China (xlichen@ieee.org, lzhh88@mail.sysu.edu.cn).

X. Xiong, X. Yan and Z. Zhu are with the School of Information Science and Technology, University of Science and Technology of China, Hefei 230027, China (zqzhu@ieee.org).

X. Chen and H. Gao are co-first authors.

Manuscript received June 5, 2023.

control plane layouts. Section IV details the principle of the composable QoT estimator and the amplifier gain optimization algorithm. We show the experimental results and the related discussions in Section V. Finally, we conclude the paper with Section VI.

II. Related Work

A. SDM Networking

SDM networks can be architected to perform switching at multiple granularity (e.g., fibers, cores and wavelengths) by trading off between node complexity and provisioning flexibility [3]. In [5], [6], the authors demonstrated switching in space, frequency and time with different bandwidth granularity leveraging 7-core fibers and a node design named Architecture on Demand. An SDM reconfigurable optical add drop multiplexer (RODAM) node capable of spatial super channel switching with a granularity of 5 Tbps was recently demonstrated over a field-deployed 15-mode MMF [7]. To effectively configure spatial super channel switching, the authors of [8] presented an SDN control plane design incorporating an SDM flow mapper and a bandwidth slicing service.

Optimizing the service provisioning in SDM networks is a challenging task owing to the increased switching dimensionality [5]–[7] and the complex physical-layer effects [4]. Routing, core and spectrum assignment (RCSA) is one of the fundamental problems in MCF SDM networks. In [10], the authors modeled the RCSA problem as an integer linear programming (ILP) formulation taking precalculated IC-XT values as constraints. In [11], the authors proposed a crosstalk-aware core and spectrum allocation policy for SDM networks. The proposed policy mitigates crosstalk by avoiding allocation of overlapping spectra in adjacent cores. This method was improved by [12] to allow certain degrees of lightpath adjacency depending on the actual crosstalk tolerance. In [13], Takeda et al. developed an RCSA algorithm for SDM elastic optical networks (EONs) taking into account both IC-XT and intra-core physical layer impairments (amplified spontaneous emission noise, etc.). While ILP formulations suffer from scalability issues, heuristic algorithms make use of artificially defined rules that can hardly capture the complex rule of SDM networks.

B. ML Applications for Optical Networks

ML has exhibited great potential in overcoming the aforementioned limitations by assisting in cognitive and autonomous networking. In [17], the authors achieved up to 99% bit error rate (BER) estimation accuracy with deep neural networks that read the wavelength loading, signal power and noise level on each link traversed by lightpaths. The work in [9] evaluated different ML algorithms for QoT estimation in SDM networks, but no feature particular to SDM was used. To reduce IC-XT in SDM networks, Klinkowski et al. leveraged ML regressors to predict the transmission distance limit of each modulation format with respect to a lightpath [23]. The authors of [28] presented a transfer learning approach for spectrum optimization in SDM EONs considering both immediate and advanced reservation connection requests.

Beside resource dimensioning, optical parameter configuration is essential for assuring desired signal QoT and thereby successful service provisioning. In [19], the authors presented a reinforcement learning algorithm that can self-learn effective launch power control policies for power excursion compensation. However, this approach induces nonnegligible training overhead and may suffer from generalization issues. An online launch power optimization design was proposed in [21], which employs a convex optimization algorithm assisted by a periodically retrained QoT estimator. Meanwhile, it has also been shown that dynamic amplifier gain control can largely mitigate optical power instability [29]. Traditional approaches for gain optimization leverage case-based reasoning [30], analytical models [31], brute-force search [32], multi-objective optimization [33], etc. In [34], the authors proposed to adjust pre-amplifier channel power utilizing ML models that predict the impact of increasing pre-amplifier power on the discrepancy of post-amplifier power.

The above proposals were mostly validated by simulations or testbed experiments. While autonomous wavelength configuration in real-world environment has been demonstrated in [20], the work introduces nonnegligible costs through repeated data plane trial and error. Moreover, autonomous provisioning over field-deployed SDM networks remains under explored.

III. Field-deployed Testbed

Fig. 1 shows the schematic of the SDM network deployed in the city of Guangzhou, China. The ring is built with four single-mode 7-core fibers of 16.5 kilometers. Six side cores are arranged hexagonally around the central core (core #4). The cladding diameter is 200 ± 5 micron and the pitch between cores is 62 ± 2 micron. Table I summarizes the physical properties of the 7-core fibers at 1550 nm. The fibers are connected every three kilometers by fusion splicing. Subject to the precision of the alignment and rotation operations and the hexagonal structure, splicing of MCFs is more difficult than that for single-mode fibers (SMFs). The splicing losses for the central and side cores average 0.04 and 0.27 dB, with the maximum values being 0.15 and 0.5 dB, respectively. The measured transmission attenuation, chromatic dispersion and IC-XT of the cores are ~ 0.2 dB/km, ~ 18.8 ps/nm/km, and < -76 dB/km, respectively. We use fan-in and fan-out (FIFO) devices to multiplex/demultiplex the cores. Specifically, we implemented the FIFO by etching and bundling seven SMFs according to the structure of the 7-core fibers. The insertion losses of the FIFO range from 0.54 to 0.9 dB for different cores. The fibers are amplified by gain-controlled erbium-doped fiber amplifiers (EDFAs) in the middle, i.e., each consists of two spans. Attributing to the diverse transmission characteristics of the cores, operating the 7-core fibers is more challenging than the management of seven parallel SMFs with relatively smaller performance variation. By cascading the fibers through the SYSU node, we implemented a four-node topology. We expect to expand the testbed with longer fibers connecting more universities/laboratories in the future. The SYSU node is equipped with 192 C-/L-band lasers, two 64-GSample/s arbitrary wavelength generators (AWGs), two

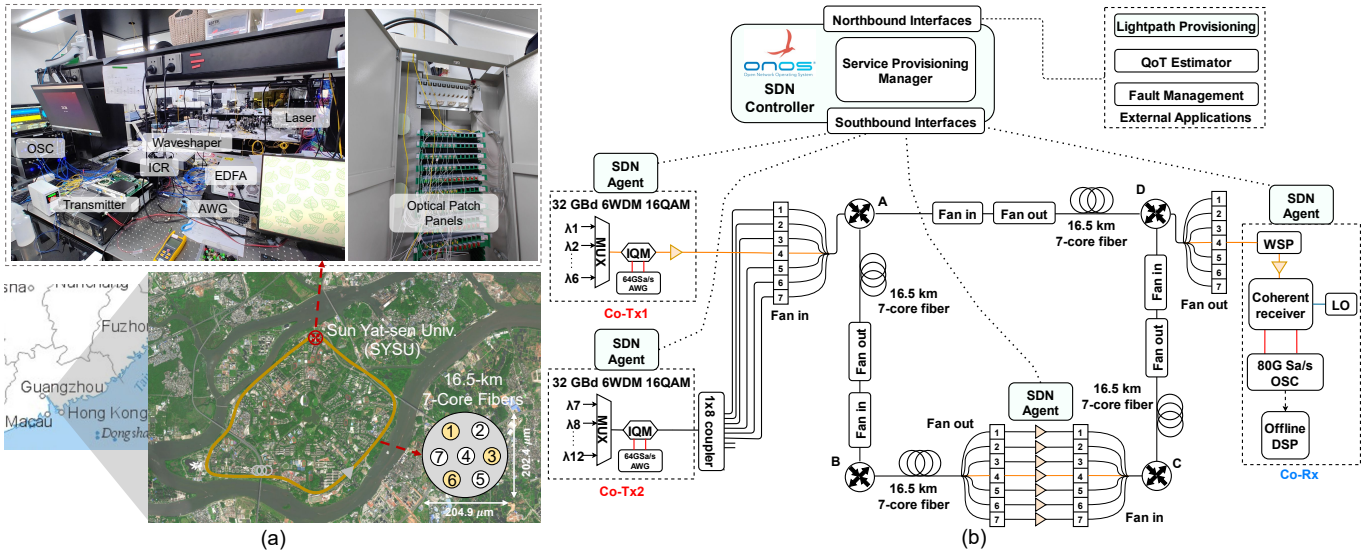

Fig. 1. Schematic of the field-deployed SDM network: (a) testbed overview; (b) control and data plane layout. OSC: oscilloscope; ICR: intradyne coherent receiver; AWG: arbitrary waveform generator; Co-Tx/-Rx: coherent transceiver/receiver; MUX: multiplexer; LO: local oscillator; IQM: in-phase/quadrature modulator; WSP: waveshaper.

TABLE I
TRANSMISSION PROPERTIES OF THE 7-CORE FIBERS.

Core ID	Splicing Loss (dB)	Attenuation (dB/km)	IC-XT (dB/km)	FIFO Insertion Loss (dB)
1	0.25	0.203	-81.8	0.71
2	0.21	0.206	-81.7	0.77
3	0.23	0.209	-83.0	0.54
4	0.04	0.207	-83.6	0.64
5	0.24	0.214	-82.4	0.78
6	0.27	0.211	-83.4	0.90
7	0.22	0.210	-83.6	0.80

IQ modulators, two coherent receivers (Co-Rxs), and one 80-GSample/s high-speed oscilloscope, which allow up to 190-channel WDM communications at 50-GHz spacing. A 4x16 waveshaper is used to perform add/drop and switching functionalities. Fig. 1(b) illustrates an exemplary experimental setup, where coherent transceiver #1 (Co-Tx1) launches six 16-QAM signals at 32 Gbauds (signals under test) into the central core. Meanwhile, Co-Tx2 injects another six dummy channels in the side cores to co-propagate with the signals under test. The signals are dropped and received by a Co-Rx after transmissions over three links.

We implemented an SDN control plane for the SDM testbed using the ONOS platform [35]. In particular, we employ a local SDN agent to manage each configurable device (EDFA, waveshaper, etc.) based on the instructions by the ONOS controller. The SDN agents also stream optical performance monitoring (OPM) data to the controller, such as the BER of a lightpath connection measured by a Co-Rx or the optical signal-to-noise ratio (OSNR) read from an optical spectrum analyzer (OSA), to enable persistent awareness of the data plane status. Inside the ONOS controller, the service provisioning manager acts as the pivot and handles various network control and management tasks, including lightpath provisioning, fault management and etc. To actuate data-driven autonomous control of the SDM network, we have developed several ML-aided applications externally. Upon triggering of an event, for instance, arrival of a lightpath request or reception of a fault alarm, the service provisioning manager calls the corresponding applications through the northbound interfaces to calculate cognitive resource allocation or equipment reconfiguration decisions. The northbound interfaces are implemented by socket connections adopting a specified protocol (message formats) momentarily, and will be upgraded to the REST API [36].

IV. AUTONOMOUS LIGHTPATH PROVISIONING DESIGN

Lightpath provisioning in SDM networks involves routing, core and spectrum assignment and necessary device configurations, particularly, tuning of amplifier gains to assure desired QoT levels for both newly established and in-service lightpaths [20], [29]. This work focuses on the optimization of amplifier gains and considers a simple shortest path routing and first-fit core/spectrum assignment policy owing to the ring-type topology used. More comprehensive resource allocation schemes that incorporate IC-XT mitigation strategies [12] can also be applied. Nonetheless, because a large number of lightpaths can interfere and compete for gains over multi-core fibers, deriving performant amplifier configurations with minimum trial and error is challenging. In this study, we extend the composable ML-based QoT estimator design proposed in [37] to the SDM context and leverage the trained modules (which compose a QoT estimator) to realize successive gain optimization for multiple amplifiers. Note that, despite the IC-XT of the deployed fibers is relatively low, performing gain optimization over the SDM network is more challenging than that over SMF networks. This is because the diverse transmission properties of the cores (as described in Section III) make core selection over the routing paths (i.e., a lightpath can traverse different cores end to end) critical in determining the physical impairments of signals and thereby the amplifier working points.

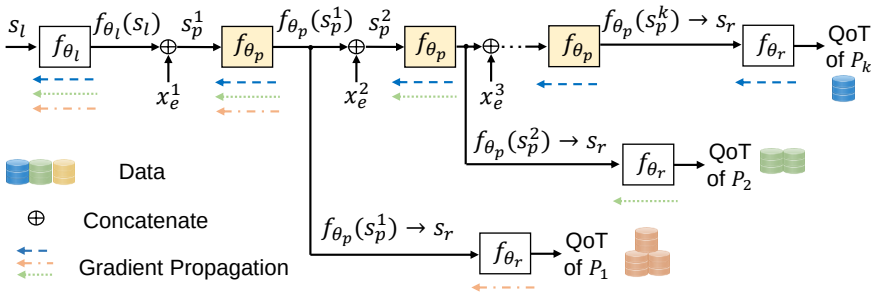

Fig. 2. Principle of composable ML-based QoT estimation.

A. QoT Estimation

A composable QoT estimator is composed of three neural network modules, namely, the *Launch*, *Propagation* and *Readout* modules. We signify the three modules by $f_{\theta_l}(s_l)$, $f_{\theta_p}(s_p)$, and $f_{\theta_r}(s_r)$, respectively, where θ_l, θ_p and θ_r represent the sets of neural network weights, s_l, s_p and s_r denote the corresponding input features. Fig. 2 shows the principle of a composable ML-based QoT estimator. The *Launch* module takes as input a lightpath's launch power, central frequency, baud rate and modulation format to model transmitter behaviors. Then, a chain of k *Propagation* modules (one for a span) are used to characterize the signal propagation process. Each *Propagation* module reads the output of the *Launch* module or that of the antecedent *Propagation* module as well as local information associated with the current span (denoted by x_e^k). Specifically, to enable capturing of the effect of IC-XT, we feature the state of a span by its core loading and amplifier gain setting. Consequently, the *Propagation* module aims at learning a mapping to a latent space that can convey the cumulative impairments of optical signals. Finally, we feed the output of the last-stage *Propagation* module to the *Readout* module to obtain the end-to-end QoT (BER, OSNR, etc.) estimation for each lightpath P_k. The composable ML method allows us to model and flexibly combine the transmission property of each core and potentially generalize the QoT estimation for lightpaths of arbitrary lengths (through adjustment of k). The design is also applicable for multi-domain (e.g., technology, vendor or administrative domains) networks provided that a proprietary set of *Launch*, *Propagation* and *Readout* modules are maintained for each domain.

The dashed/dotted lines in Fig. 2 show the training pipeline. We apply an end-to-end training mechanism [37] that trains the three modules jointly according to the chain rule. Specifically, given a data batch $\mathbb{D}$, the gradients of the loss function $L_{\mathbb{D}}(\theta_l, \theta_p, \theta_r)$ (e.g., mean squared error) with respect to θ_l can be obtained by,

$$\frac{\partial L_{\mathbb{D}}}{\partial \theta_l} = \frac{1}{|\mathbb{D}|} \sum_{d_i \in \mathbb{D}} \frac{\partial L_{d_i}}{\partial f_{\theta_l}(s_l)} \frac{\partial f_{\theta_l}(s_l)}{\partial \theta_l} \Big|_{f_{\theta_l}(s_l)=f_{\theta_l}(s_l^i), s_l^i \in d_i}, \quad (1)$$

where $|\mathbb{D}|$ represents the size of $\mathbb{D}$.

B. Amplifier Gain Configuration

Let $A = \{A_n\}|_{n\in[1,N]}$ denote the set of amplifiers to be configured during lightpath provisioning. The gain of each amplifier A_n can be adjusted by configuration of its input current from a set of discrete values $G = \{G_0 + m \cdot \Delta\}|_{m\in[0,M-1]}$ with a granularity of Δ. This leads to an exponentially scaling solution space, i.e., M^N solutions totally. In pursuit of time-efficient amplifier configuration, we exploit the composable QoT estimator's capability of per-span impairment assessment and develop a greedy approach that performs sequential optimization for each A_n.

Algorithm 1: Composable ML-aided amplifier gain optimization algorithm.

Input: A, G, f_{θ_l}, f_{θ_p}, f_{θ_r}, set of lightpaths P
Output: optimized gain g_n^* for each $A_n \in A$, $g_n^* \in G$

1 **for** *each* $A_n \in A$ **do**
  `// traverse feasible configurations`
2 **for** *each* $G_m \in G$ **do**
3 construct local features x_e^n based on G_m;
4 **for** *each lightpath* P_w *in the span* **do**
5 calculate $\hat{f}^w = f_{\theta_l}(s_l^w)$ or $f_{\theta_p}(s_p^{w,k_w-1})$;
6 $s_p^{w,k_w} = \{\hat{f}^w, x_e^n\}$;
  `// estimate the BER of` P_w
7 $b^{w,k_w} = f_{\theta_r}(f_{\theta_p}(s_p^{w,k_w}))$;
8 **end**
  `// score` G_m `by BER margins`
9 **if** $\exists b^{w,k_w} > b_{th}$ **then**
10 $c_m = -1$;
11 **else**
12 $c_m = \sum_{P_w}(|P_w| - k_w)\log(b_{th} - b^{w,k_w} + 1)$;
13 **end**
14 **end**
15 **if** $\max_m c_m < 0$ **then**
16 mark failure of lightpath provisioning;
17 **return**;
18 **end**
19 $g_n^* = \arg\max_{G_m} c_m$;
20 **end**

Algorithm 1 summarizes the procedures of the algorithm. Lines 1-20 cover the sequential optimization procedure for amplifiers ordered in accordance to the direction of signal propagation. For each amplifier, we traverse every feasible

configuration G_m and estimate the overall QoT margins that can be obtained with G_m (lines 2-14). In particular, we call the trained *Launch*, *Propagation* and *Readout* modules to estimate the BER of each lightpath in the span. Line 5 retrieves the output of the *Launch* module for the first span (regarding the current lightpath) or that of the antecedent *Propagation* module otherwise. Line 6 constructs an input for the *Propagation* module by concatenating the local features and the output of the previous module. Next, in line 7, we assess the QoT of a connection with the *Readout* module even if the lightpath does not terminate immediately. Lines 9-13 score G_m based on the BER margin. If G_m leads to BER dissatisfaction for any of the lightpaths, a negative score is assigned with line 10. Otherwise, G_m is scored by the total BER margin weighted by the number of spans remaining for each lightpath, i.e., $|P_w| - k_w$ (line 12). Here, $|P_w|$ returns the total number of spans of lightpath P_w, while k_w represents the position of the current span in P_w. By the equation in line 12, we prioritize configurations resulting in bigger BER budgets for signals having more spans yet to propagate. Note that, instead of using such an empirical policy, one can leverage the recent advances in deep reinforcement learning [38] to parameterize and learn more sophisticated scoring functions. Finally, if there exists at least one viable configuration (i.e., the QoT target is met for all the lightpaths), line 19 picks the solution with the highest score. Otherwise, the provisioning of the new lightpaths is declined (lines 16-17). We can see that the composable QoT estimator trained essentially functions as a digital twin of optical signal transmission, allowing the proposed algorithm to compute the target amplifier configurations in one shot without data plane trial and error. Thus, the interference in the in-service connections can be significantly reduced.

V. Experimental Results

We implemented the aforementioned algorithm and demonstrated autonomous lightpath provisioning over the field-deployed SDM testbed described in Section III.

A. Training of QoT Estimator

We first trained a composable QoT estimator with experimental data collected from the SDM network. To cover diversified network conditions, we set up lightpaths operating at different rates (32/20/16 Gbauds) adopting either the 16-QAM or QPSK modulation. The loading of each core in a fiber link was changed by injection of a different number of dummy channels. We performed input current sweeping (45−220 mA) for each EDFA to assess the impact of amplifier gain on signal QoT, exploring both the linear and nonlinear regimes. Fig. 3(a) shows the nonlinear effects observed in the experiments. Overall, we collected $4,965$ data instances, which were then divided into a training and a testing set according to a ratio of $8:2$.

We implemented the *Launch*, *Propagation* and *Readout* modules all with neural network blocks of two fully-connected layers. Each layer takes *ReLU* as the activation function except for the output layer of the *Readout* module. Fig. 3(b) shows the evolution of training and validation losses. Both losses converged after training of 600 epochs, indicating good fitting of the modules. Ultimately, the QoT estimator could achieve a BER (in a logarithmic scale) prediction accuracy of $\sim 96.1\%$ on the testing set.

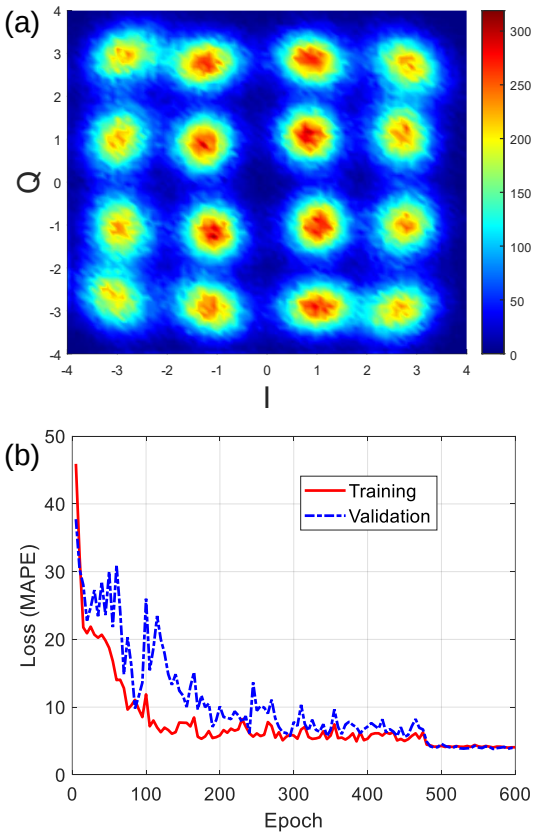

Fig. 3. (a) Nonlinear effects observed in the experiments, and (b) evolution of training and validation losses.

B. Amplifier Gain Configuration

Next, we conducted autonomous lightpath configuration experiments. Fig. 4(a) presents the Wireshark capture of control plane message exchanges during provisioning of a connection. It took the lightpath provisioning application (running on a PC equipped with an AMD Ryzen7 5800 8-core processor and 16-GB memory) 6.74 seconds to return an EDFA configuration scheme, which was then successfully applied after another 1.07 seconds. We expect the configuration process can be effectively accelerated pending more computing power and parallel computing being adopted. Figs. 4(b) and (c) show the detail of a service request and a configuration command captured. The request message conveys key information of a connection to be set up, while the configuration command informs that the current of the EDFA should be set to 65 mA.

We show case the EDFA currents and the corresponding BER of five wavelengths in one of the cores before and after configuration in Fig. 5. Other cores were filled with dummy wavelengths. All the wavelengths used the 16-QAM modulation. Fig. 5(a) shows that one connection at 193.15 THz was operating correctly initially, with the currents of the two EDFAs traversed being set to 90 and 80 mA respectively (top). After four new wavelengths were launched, the BER of

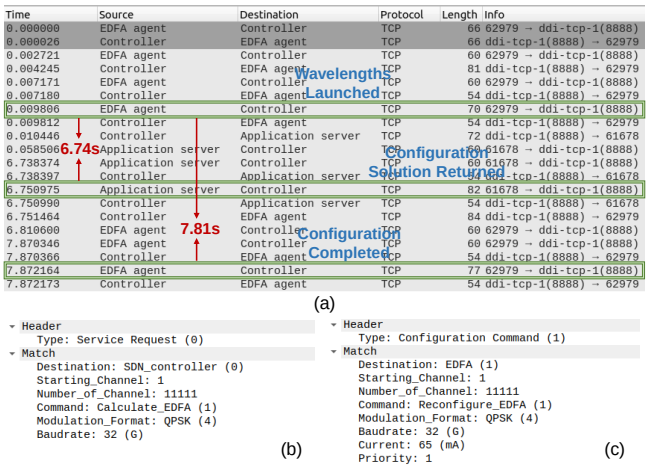

Fig. 4. (a) Control plane message exchanges during lightpath provisioning, and examples of (b) service request and (c) configuration command messages.

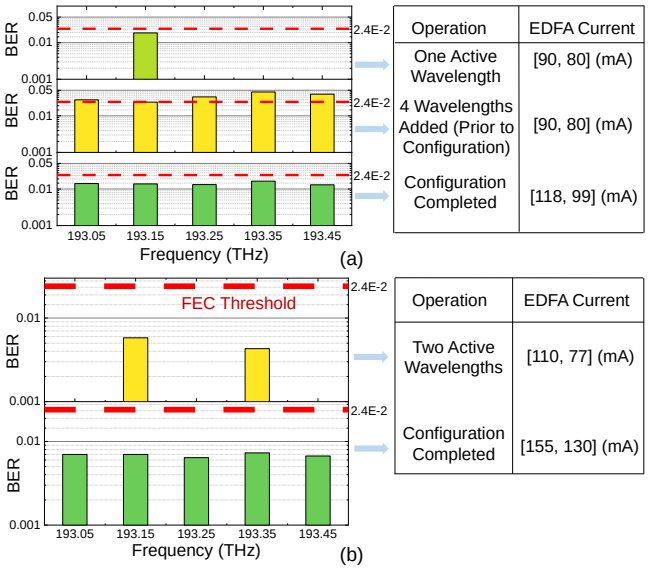

Fig. 5. EDFA currents and the corresponding BER performance before and after configuration for (a) 32-Gbaud and (b) 20-Gbaud signals (16-QAM modulation for both cases).

all five wavelengths went above the forward error correction (FEC) threshold under the same EDFA configuration (middle). With the proposed algorithm, we adjusted the currents of the two EDFAs to be 118 and 99 mA, assuring the QoT requirement for every signal was satisfied (bottom). Similar results were obtained with a decreased rate of 20 Gbauds (see Fig. 5(b)). After the injection of three wavelengths, we retuned the EDFA currents from 100 and 77 mA to 155 and 130 mA, respectively, so that all the BER values were below the FEC threshold. We also tested the cases when the QPSK modulation was applied to 32-/16-Gbaud signals and plotted the results in Fig. 6. Three EDFAs were involved in both cases. After reconfiguration of the EDFAs with the assist of the proposed algorithm, the BER performance of all in-service and newly established wavelengths unanimously improved to below the FEC threshold. One can observe from Figs. 5 and 6 that the proposed algorithm suggested larger currents for 16-QAM signals compared with QPSK signals. We attribute

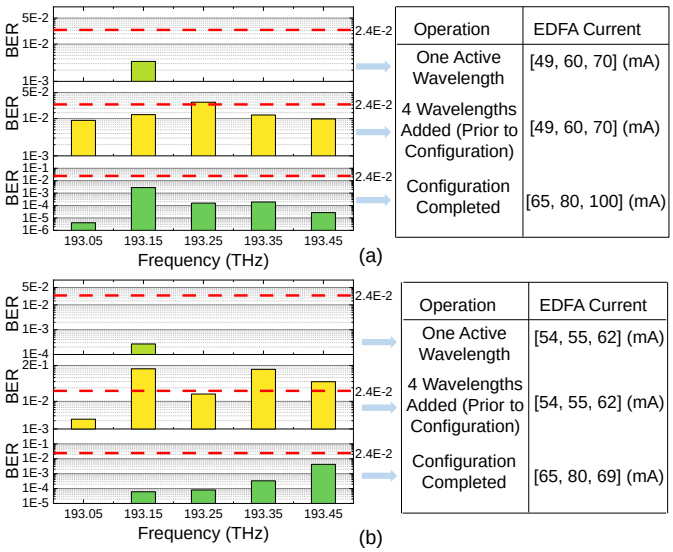

Fig. 6. EDFA currents and the corresponding BER performance before and after configuration for (a) 32-Gbaud and (b) 16-Gbaud signals (QPSK modulation for both cases).

this to the higher ONSR requirements by 16-QAM signals [39]. Also, the results indicate larger currents were used for 20-Gbaud signals with respect to 32-Gbaud signals when the 16-QAM modulation was adopted. Whereas, this was not the situation for QPSK signals. We presume that this is because 16-QAM signals suffer from more severe nonlinear effects at higher baud rates, discouraging the use of higher gains.

C. Failover

Lastly, we demonstrated automated failover with two failure scenarios. In the first scenario, we selected a 32-Gbaud signal transmitted in the central core (core #4) as the testing signal. The coherent receiver constantly monitored the BER of the signal as shown by Fig. 7. We artificially removed a flange along the routing path at a certain point to emulate equipment malfunctioning, which caused a quick deterioration of the signal QoT. The system detected the violation of the FEC threshold and reconfigured the waveshaper to switch the wavelength to a side core (core #1). The failover process took 10.5 seconds, where after, the signal BER restored to an acceptable level.

In the second scenario, we introduced receiver filter shifting by changing the filter central frequency from 193.053 THz to 193.083 THz. Fig. 8 shows the signal spectrogram captured during the experiment. The rightmost spectrum became noisy due to the filter shifting (middle). We made use of an optical spectrometer to continuously monitor the OSNR of the connection. When the system identified that the OSNR value dropped to below a threshold (see Fig. 9), it configured the waveshaper to bypass the faulty filter. Afterward, the OSNR returned to above the threshold. The restoration was completed in 11.8 seconds. Note that, in the aforementioned proof-of-concept experiments, we had applied a simple threshold-based fault detection policy and omitted the fault identification and localization procedures. Our future work will devote to close the loop by exploring more failure scenarios (e.g., amplifier

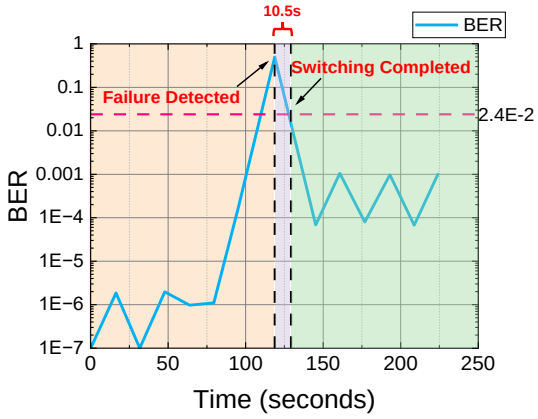

Fig. 7. BER monitoring in the first failover scenario.

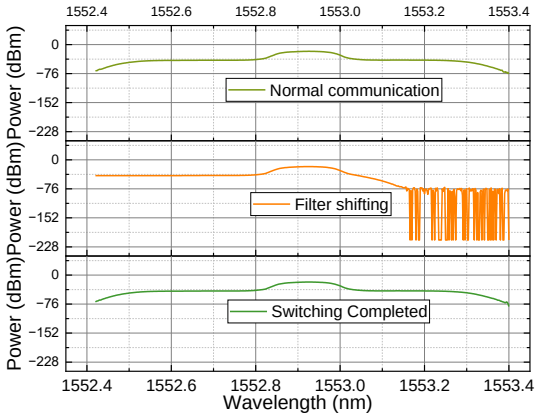

Fig. 8. Received spectra in the second failover scenario.

malfunctioning, physical-layer attacks, misconfigurations, filter narrowing) and deploying more powerful fault management applications [24]–[26]. For instance, we could exploit the hybrid learning approach presented in [26] which makes use of a clustering algorithm to learn fault patterns beyond normal network fluctuations to avoid excessive path switching.

VI. Conclusion

In this paper, we demonstrated autonomous lightpath provisioning over a field-deployed SDM network using 7-core fibers. We proposed a sequential amplifier gain optimization algorithm taking advantage of a composable QoT estimator. Autonomous lightpath provisioning and failover experiments under various scenarios verify the effectiveness of the proposed design. Our future work includes: (*i*) expanding the SDM testbed with more nodes in mess topologies and large-scale wavelength/core switching capabilities; (*ii*) investigating more comprehensive routing, core and spectrum assignment policies; and (*iii*) studying ML designs for cognitive fault detection, identification and localization in SDM networks.

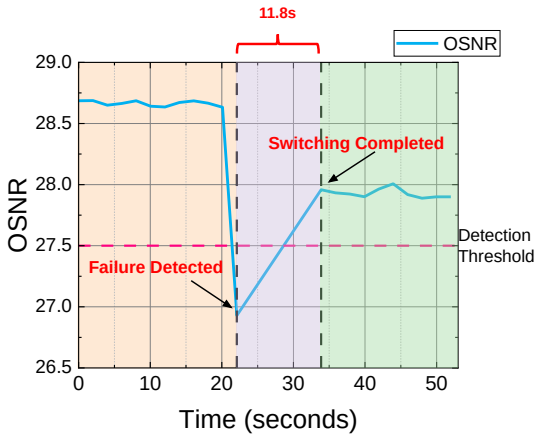

Fig. 9. OSNR monitoring in the second failover scenario.

Acknowledgment

This work was supported in part by NSFC under Project 62201627, Guangzhou Basic and Applied Basic Research Foundation (No. SL2022A04J01907), the Guangdong Program (No. 2021QN02X039), and Innovation Group Project of Southern Marine Science and Engineering Guangdong Laboratory (Zhuhai) (No. SML2022007).

References

[1] R. Proietti, L. Liu, R. P. Scott, B. Guan, C. Qin, T. Su, F. Giannone, and S. J. B. Yoo, "3d elastic optical networking in the temporal, spectral, and spatial domains," *IEEE Commun. Mag.*, vol. 53, no. 2, pp. 79–87, 2015.

[2] G. Rademacher, B. J. Puttnam, and R. S. Luis, "10.66 peta-bit/s transmission over a 38-core-three-mode fiber," in *Proc. Conf. Opt. Fiber Commun.*, 2020, paper Th3H.1.

[3] D. M. Marom, Y. Miyamoto, D. T. Neilson, and I. Tomkos, "Optical switching in future fiber-optic networks utilizing spectral and spatial degrees of freedom," *Proc. of the IEEE*, vol. 110, no. 11, pp. 1835–1852, 2022.

[4] N. Sambo, C. Lasagni, P. Serena, P. Castoldi, and A. Bononi, "Impact of the interplay between mode dispersion and kerr effect in SDM optical networks," *J. Lightw. Technol.*, vol. 41, no. 6, pp. 1603–1609, 2023.

[5] N. Amaya, M. Irfan, G. Zervas, R. Nejabati, D. Simeonidou, J. Sakaguchi, W. Klaus, B. J. Puttnam, T. Miyazawa, Y. Awaji, N. Wada, and I. Henning, "First fully-elastic multi-granular network with space/frequency/time switching using multi-core fibres and programmable optical nodes," in *Proc. Eur. Conf. Opt. Commun.*, 2012, th.3.D.3.

[6] ——, "Fully-elastic multi-granular network with space/frequency/time switching using multi-core fibres and programmable optical nodes," *Opt. Express*, vol. 21, no. 7, pp. 8865–8872, 2013.

[7] R. S. Luis, G. Rademacher, B. J. Puttnam, G. Di Sciullo, A. Marotta, R. Emmerich, N. Braig-Christophersen, R. Stolte, F. Graziosi, A. Mecozzi, C. Schubert, G. Ferri, F. Achten, P. Sillard, R. Ryf, L. Dallachiesa, S. Shinada, C. Antonelli, and H. Furukawa, "Demonstration of a spatial super channel switching SDM network node on a field deployed 15-mode fiber network," in *Proc. Eur. Conf. Opt. Commun.*, 2022, th3C.5.

[8] N. Amaya, S. Yan, M. Channegowda, B. R. Rofoee, Y. Shu, M. Rashidi, Y. Ou, E. Hugues-Salas, G. Zervas, R. Nejabati, D. Simeonidou, B. J. Puttnam, W. Klaus, J. Sakaguchi, T. Miyazawa, Y. Awaji, H. Harai, and N. Wada, "Software defined networking (SDN) over space division multiplexing (SDM) optical networks: features, benefits and experimental demonstration," *Opt. Express*, vol. 22, no. 3, pp. 3638–3647, 2014.

[9] C. Manso, R. Vilalta, R. Munoz, N. Yoshikane, R. Casellas, R. Martinez, C. Wang, F. Balasis, T. Tsuritani, and I. Morita, "Scalability analysis of machine learning QoT estimators for a cloud-native SDN controller on a WDM over SDM network," *J. Opt. Commun. Netw.*, vol. 14, no. 4, pp. 257–266, 2022.

[10] C. Rottondi, P. Martelli, P. Boffi, L. Barletta, and M. Tornatore, "Crosstalk-aware core and spectrum assignment in a multicore optical link with flexible grid," *IEEE Trans. Commun.*, vol. 67, no. 3, pp. 2144–2156, 2019.

[11] S. Fujii, Y. Hirota, H. Tode, and K. Murakami, "On-demand spectrum and core allocation for reducing crosstalk in multicore fibers in elastic optical networks," *J. Opt. Commun. Netw.*, vol. 6, no. 12, pp. 1059–1071, 2014.

[12] Y. Seki, Y. Tanigawa, Y. Hirota, and H. Tode, "Core and spectrum allocation to achieve graceful degradation of inter-core crosstalk with generalized hierarchical core prioritization on space-division multiplexing elastic optical networks," *J. Opt. Commun. Netw.*, vol. 15, no. 1, pp. 43–56, 2023.

[13] K. Takeda, T. Sato, B. C. Chatterjee, and E. Oki, "Joint inter-core crosstalk- and intra-core impairment-aware lightpath provisioning model in space-division multiplexing elastic optical networks," *IEEE Trans. Netw. Service Manag.*, vol. 19, no. 4, pp. 4323–4337, 2022.

[14] X. Chen, R. Proietti, H. Lu, A. Castro, and S. J. B. Yoo, "Knowledge-based autonomous service provisioning in multi-domain elastic optical networks," *IEEE Commun. Mag.*, vol. 56, no. 8, pp. 152–158, Aug. 2018.

[15] L. Gitre, C. Natalino, S. Gonzalez-Diaz, F. Soldatos, S. Barguil, C. Aslanoglou, F. J. Moreno-Muro, A. N. Q. Cornelio, L. Cepeda, R. Martinez, C. Manso, V. Apostolopoulos, S. P. Valiviita, O. G. de Dios, J. Rodriguez, R. Casellas, P. Monti, G. P. Katsikas, R. Muñoz, and R. Vilalta, "Demonstration of zero-touch device and l3-VPN service management using the teraflow cloud-native SDN controller," in *Proc. Conf. Opt. Fiber Commun.*, 2022, paper M3Z.15.

[16] J. Yu, W. Mo, Y. Huang, E. Ip, and D. C. Kilper, "Model transfer of QoT prediction in optical networks based on artificial neural networks," *J. Opt. Commun. Netw.*, vol. 11, no. 10, pp. C48–C57, 2019.

[17] C. Liu, X. Chen, R. Proietti, and S. J. B. Yoo, "Evol-TL: Evolutionary transfer learning for QoT estimation in multi-domain networks," in *Proc. Conf. Opt. Fiber Commun.*, 2020, paper Th3D.1.

[18] D. Sequeira, M. Ruiz, N. Costa, A. Napoli, J. Pedro, and L. Velasco, "OCATA: a deep-learning-based digital twin for the optical time domain," *J. Opt. Commun. Netw.*, vol. 15, no. 2, pp. 87–97, 2023.

[19] M. Freire-Hermelo, D. Sengupta, A. Lavignotte, C. Tremblay, and C. Lepers, "Reinforcement learning for compensating power excursions in amplified WDM systems," *J. Lightw. Technol.*, vol. 39, no. 21, pp. 6805–6813, 2021.

[20] Z. Zhong, M. Ghobadi, M. Balandat, S. Katti, A. Kazerouni, J. Leach, M. McKillop, and Y. Zhang, "BOW: First real-world demonstration of a bayesian optimization system for wavelength reconfiguration," in *Proc. Conf. Opt. Fiber Commun.*, 2021, f3B.1.

[21] A. Mahajan, K. Christodoulopoulos, R. Martinez, R. Munoz, and S. Spadaro, "Quality of transmission estimator retraining for dynamic optimization in optical networks," *J. Opt. Commun. Netw.*, vol. 13, no. 4, pp. B45–B59, 2021.

[22] B. Li, W. Lu, and Z. Zhu, "Deep-NFVOrch: leveraging deep reinforcement learning to achieve adaptive vNF service chaining in DCI-EONs," *J. Opt. Commun. Netw.*, vol. 12, no. 1, pp. A18–A27, Jan. 2020.

[23] M. Klinkowski, P. Ksieniewicz, M. Jaworski, G. Zalewski, and K. Walkowiak, "Machine learning assisted optimization of dynamic crosstalk-aware spectrally-spatially flexible optical networks," *J. Lightw. Technol.*, vol. 38, no. 7, pp. 1625–1635, 2020.

[24] D. Rafique, T. Szyrkowiec, H. Grießer, A. Autenrieth, and J. Elbers, "Cognitive assurance architecture for optical network fault management," *J. Lightw. Technol.*, vol. 36, no. 7, pp. 1443–1450, Apr. 2018.

[25] M. Furdek, C. Natalino, A. Di Giglio, and M. Schiano, "Optical network security management: requirements, architecture, and efficient machine learning models for detection of evolving threats [invited]," *J. Opt. Commun. Netw.*, vol. 13, no. 2, pp. A144–A155, 2021.

[26] X. Chen, C. Liu, R. Proietti, Z. Li, and S. J. B. Yoo, "Automating optical network fault management with machine learning," *IEEE Commun. Mag.*, vol. 60, no. 12, pp. 88–94, 2022.

[27] H. Gao, X. Chen, W. Zheng, Y. Chen, Y. Xiao, and Z. Li, "Demonstration of composable-ML-assisted autonomous lightpath configuration over a field-deployed SDM network with 7-core fibers," in *Proc. Conf. Opt. Fiber Commun.*, 2023, paper Th4C.2.

[28] Q. Yao, H. Yang, A. Yu, and J. Zhang, "Transductive transfer learning-based spectrum optimization for resource reservation in seven-core elastic optical networks," *J. Lightw. Technol.*, vol. 37, no. 16, pp. 4164–4172, 2019.

[29] Y. Li and D. C. Kilper, "Optical physical layer SDN [invited]," *J. Opt. Commun. Netw.*, vol. 10, no. 1, pp. A110–A121, 2018.

[30] U. Moura, M. Garrich, H. Carvalho, M. Svolenski, A. Andrade, F. Margarido, A. C. Cesar, E. Conforti, and J. Oliveira, "SDN-enabled EDFA gain adjustment cognitive methodology for dynamic optical networks," in *Proc. Eur. Conf. Opt. Commun.*, 2015, pp. 1–3.

[31] K. B. Roberts, J. Harley, and D. Boertjes, "Adjustment of control parameters of section of optical fiber network," US Patent, US10236981B2.

[32] B. Correia, R. Sadeghi, E. Virgillito, A. Napoli, N. Costa, J. Pedro, and V. Curri, "Power control strategies and network performance assessment for C+L+S multiband optical transport," *J. Opt. Commun. Netw.*, vol. 13, no. 7, pp. 147–157, 2021.

[33] E. A. Barboza, C. J. A. Bastos-Filho, and J. F. M. Filho, "Adaptive control of optical amplifier operating point using VOA and multi-objective optimization," *J. Lightw. Technol.*, vol. 37, no. 16, pp. 3994–4000, 2019.

[34] Y. Huang, P. B. Cho, P. Samadi, and K. Bergman, "Dynamic power pre-adjustments with machine learning that mitigate EDFA excursions during defragmentation," in *Proc. Conf. Opt. Fiber Commun.*, 2017, th1J.2.

[35] Open network operating system (ONOS) SDN controller for SDN/NFV solutions. [Online]. Available: https://opennetworking.org/onos/

[36] Rest API tutorial. [Online]. Available: https://www.restapitutorial.com/index.html

[37] H. Gao, X. Chen, L. Sun, and Z. Li, "CompQoTE: Generalizing QoT estimation with composable ML and end-to-end learning," in *Proc. Conf. Opt. Fiber Commun.*, 2023, paper W4G.1.

[38] M. Raza, C. Natalino, P. Öhlen, L. Wosinska, and P. Monti, "Reinforcement learning for slicing in a 5G flexible RAN," *J. Lightw. Technol.*, vol. 37, no. 20, pp. 5161–5169, Oct. 2019.

[39] R. Proietti, X. Chen, K. Zhang, G. Liu, M. Shamsabardeh, A. Castro, L. Velasco, Z. Zhu, and S. J. B. Yoo, "Experimental demonstration of machine-learning-aided QoT estimation in multi-domain elastic optical networks with alien wavelengths," *J. Opt. Commun. Netw.*, vol. 11, no. 1, pp. A1–A10, 2019.